

ON THE HIGH WEISSENBERG NUMBER PROBLEM

ROLAND KEUNINGS

*Center for Advanced Materials, Lawrence Berkeley Laboratory, University of California,
Berkeley, CA 94720 (U.S.A)*

(Received September 12, 1985; in revised form December 13, 1985)

Summary

We address the outstanding problem affecting the numerical simulation of steady viscoelastic flows in complex geometries, namely the existence of a critical value of the Weissenberg number beyond which no discrete solutions can be obtained. The flow of Maxwell and Leonov-like fluids through a sudden contraction is selected as a test problem. Discrete solutions are obtained by means of a mixed Galerkin/Finite Element method. We find that limit points of the discrete solution families are responsible for the loss of convergence of the iterative scheme. Intensive mesh refinement shows, however, that these limit points are numerical artifacts.

1. Introduction

It has been recognized for several years that the numerical computation of non-trivial viscoelastic flows is a very challenging enterprise. Ever since the early attempts of the mid 1970's, researchers have repeatedly met with an outstanding problem, namely the failure of their numerical schemes to provide solutions beyond some critical value of the Weissenberg number, a dimensionless group that determines the elastic character of the flow. Often referred to in the literature as the *high Weissenberg number problem*, this major difficulty has been the central theme of the previous Workshops on Numerical Simulation of Viscoelastic Flows (see the editorials [1,2] and the reviews [3,4]).

Computing the flow of a viscoelastic fluid in a complex geometry requires the solution of a set of non-linear partial differential (or possibly integro-differential) equations consisting of the conservation laws and a specific constitutive model. For isothermal flows, the unknown fields are typically the velocity, pressure, and extra-stress fields. We shall refer to this set of equations and the possible solutions as the continuous problem and the

exact solutions, respectively. Exact solutions cannot be obtained in most cases, and one has to resort to numerical solution procedures. A discretization method is used to transform the continuous problem into a set of non-linear algebraic equations; * this set is solved iteratively in terms of unknown coefficients that define an approximation of an exact solution. We shall refer to this set of equations and the possible solutions as the discrete problem and the discrete solutions, respectively.

It is relevant to wonder whether the high Weissenberg number problem would not reflect some qualitative property of the continuous problem. In order to illustrate this point, let us consider the test problem of steady two-dimensional axisymmetric flow of a Maxwell fluid through a sudden contraction. Here, the Weissenberg number We is defined as the product of the relaxation time of the material and the wall shear rate in the downstream fully developed flow. Suppose that we can calculate exact solutions. Starting from the Newtonian result ($We = 0$), we wish to compute an exact solution family parameterized by We . One of the following cases will apply **:

(A) The solution family emanating from the Newtonian solution exists and is stable whatever the value of We .

(B) The solution family becomes unstable beyond a critical value We_{crit} , although it continues to exist.

(C) The solution family terminates abruptly at a critical value We_{crit} .

(D) The solution family has a limit point at a critical value We_{crit} and turns back on itself towards decreasing We .

Case A is very unlikely to occur, since we are dealing with a highly non-linear system. Case B would indicate that steady two-dimensional axisymmetric flows of a Maxwell fluid cannot be maintained beyond We_{crit} in the present geometry. Case C would mean that flows of the assumed type do not exist for $We > We_{crit}$, at least in the solution family emanating from the Newtonian solution. Case D would not necessarily imply the loss of flow fields of the assumed type beyond We_{crit} ; indeed, another limit point might be encountered on the return solution branch, after which the solution family would turn again towards increasing We . Note that bifurcation to flows of a different type (three-dimensional steady, for example) might ensue at We_{crit} in cases B, C, and D.

Let us consider now a discrete version of the same problem. Assuming that we know which of the four cases A to D applies to the exact solution family, can we infer therefrom the corresponding qualitative behavior of the discrete solution family? There is no general answer to this question. A

* Here we consider steady flows; only a few transient viscoelastic flows in complex geometries have been studied so far (see e.g. [4-7]).

** We assume that continuation from the Newtonian solution is possible.

conservative approach, which as we shall see turns out to be a realistic one in the context of viscoelastic flow computations, is to recognize that no guarantee exists that the qualitative properties stated in cases A to D will be transferred without alteration from the continuous level to the discrete level.

These considerations are more than mathematical issues for purists. Indeed, recent work has clearly identified the occurrence of limit points in the discrete solution families of certain viscoelastic flow problems [8,9]. This result is highly significant in that it explains *per se* the loss of convergence of conventional iterative schemes beyond the limit point. We believe, however, that the critical question raised earlier has not been answered unequivocally: are these limit points numerical artifacts or do they translate an intrinsic property of the continuous problem? The purpose of the present paper is to address this issue.

We describe hereafter new results for steady two-dimensional flows of Maxwell and Leonov-like fluids through a planar sudden contraction. Both fluids are particular cases of the constitutive model developed by Giesekus [10]. The numerical technique used in the present work is an extension of a mixed Galerkin/Finite Element technique referred to as algorithm MIX1 in our previous publications (e.g. see [11]). We combine a Newton–Raphson iterative scheme with a first-order continuation procedure to compute discrete solution families parameterized by the Weissenberg number.

The results show that limit points in the discrete solution families are responsible for the high Weissenberg number problem. This confirms the conclusions of [8,9] based on other flow problems and different numerical techniques. A very intensive mesh refinement study demonstrates, however, that these limit points are not intrinsic features of the continuous problem, but rather have a numerical origin. These conclusions are drawn with both Maxwell and Leonov-like fluids, although the actual behavior of the numerical scheme is drastically different from one case to the other. Finally, a numerical experiment conducted with the Maxwell fluid shows the limitations of the present Galerkin formulation and points to the need for improved discretization procedures. Preliminary results of the present study have been described in [12].

2. Test problem: formulation and numerical method

The constitutive model developed by Giesekus [10] for modeling polymeric solutions and melts can be written as

$$\boldsymbol{\sigma} = -p\mathbf{I} + \mathbf{T}_p + \mathbf{T}_s, \quad (1)$$

$$\left[\mathbf{I} + \alpha \frac{\lambda}{\mu_p} \mathbf{T}_p \right] \mathbf{T}_p + \lambda \overset{\nabla}{\mathbf{T}}_p = 2\mu_p \mathbf{D}, \quad (2)$$

$$\mathbf{T}_s = 2\mu_s \mathbf{D}. \quad (3)$$

Here, σ denotes the Cauchy stress tensor, which is decomposed into an indeterminate pressure term $-pI$, a polymer contribution T_p , and a Newtonian solvent contribution T_s . I denotes the unit tensor, D is the rate of strain tensor, and the superscript ∇ stands for the upper-convected derivative. The parameters μ_p and μ_s are constant viscosity coefficients, λ is a zero-shear relaxation time, and α denotes Giesekus's mobility parameter ($0 \leq \alpha \leq 1$).

Limiting cases of the Giesekus model include the Newtonian fluid ($\alpha = \lambda = 0$), the upper-convected Maxwell fluid ($\alpha = \mu_s = 0$), the Oldroyd-B fluid ($\alpha = 0$), and the Leonov-like model ($\alpha = 0.5$). The latter duplicates the Leonov fluid [13] in simple shear flows only. The Giesekus model with $\alpha > 0$ predicts a shear-thinning viscosity and non-vanishing first and second normal stress differences in viscometric flows, a finite extensional viscosity for all values of the extensional rate, and stress-overshoot in start-up flows [10,14].

We consider here steady isothermal flows, in which case the conservation laws reduce to

$$\nabla \cdot \sigma = 0, \quad (4)$$

$$\nabla \cdot v = 0, \quad (5)$$

where v is the velocity vector. We have neglected convective and body force terms in the momentum equation (4), and have assumed that the fluid is incompressible.

We solve the set of governing equations (1–5) by means of a mixed Galerkin/Finite Element technique originally developed for the case of the Maxwell fluid [15,16] and further extended to the Oldroyd-B and Phan Thien–Tanner fluids [11,17,18]. Briefly, we define standard finite element approximations for the elastic stress T_p , the velocity vector v , and the pressure p as follows

$$T_p^* = \sum_{i=1}^M T_p^i \psi_i, \quad v^* = \sum_{i=1}^M v^i \psi_i, \quad p^* = \sum_{j=1}^N p^j \phi_j, \quad (6)$$

where T_p^i , v^i , p^j are unknown nodal coefficients, and ψ_i , ϕ_j are given shape functions. Application of the Galerkin method to the governing equations (1–5) yields

$$\langle \psi_i; \left[I + \alpha \frac{\lambda}{\mu_p} T_p^* \right] T_p^* + \lambda \overset{\nabla}{T}_p^* - 2\mu_p D^* \rangle = 0, \quad (7)$$

$$\langle (\nabla \psi_i)^T; -p^* I + 2\mu_s D^* + T_p^* \rangle = f^i, \quad (8)$$

$$\langle \phi_j; \nabla \cdot v^* \rangle = 0, \quad (9)$$

with $1 \leq i \leq M$ and $1 \leq j \leq N$; f^i denotes the generalized nodal force at node i , and the angular brackets $\langle ; \rangle$ stand for the L^2 -scalar product. We use 9-node quadrilateral and 6-node triangular isoparametric elements to discretize the flow domain; the shape functions for the velocity and extra-stress fields are P^2-C^0 polynomials, while those for the pressure field are P^1-C^0 polynomials. Implementation details are given in [4] for the particular cases of Maxwell and Oldroyd-B fluids.

We consider in the present paper steady two-dimensional flows through a 4:1 planar sudden contraction. The boundary conditions are: (i) fully developed velocity and elastic extra-stress fields at the upstream section, (ii) no-slip at the wall of the contraction, (iii) fully developed velocity field at the downstream section, and (iv) symmetry conditions at the plane of symmetry. Three dimensionless groups arise in the present application: the mobility coefficient α , the viscosity ratio $\beta = \mu_s/(\mu_s + \mu_p)$, and the Weissenberg number $We = \lambda V/H$ (here, V is the average velocity in the downstream slit of half-thickness H).

Equations (7–9) constitute a set of non-linear algebraic equations depending on the three parameters α , β , and We . For fixed values of α and β , we compute a solution family parameterized by We by means of the Newton–Raphson iterative scheme, starting from the Newtonian solution ($We = 0$). We use a first-order continuation strategy to obtain initial estimates for the Newton iterations. This procedure produces quadratically convergent iterates as long as the Jacobian matrix remains regular and sufficiently small increments in We are used. When a limit point is reached, convergence of the non-linear iterations is lost, the Jacobian matrix becomes singular, and arc-length continuation techniques must be devised if one wishes to compute the return branch (see e.g. [8]). In the present work, we are mainly interested in the *location* in the parameter space of the *first* limit point in the solution family emanating from the Newtonian solution.

Figures 1 and 2 show the five finite element meshes used in the calculations; characteristic data of these meshes are listed in Table 1. Meshes M1, M2, and M3 have been used in [18] for the study of entry flows of a Phan Thien–Tanner fluid, while M4 and M5 have been specially designed for the purpose of the present mesh refinement analysis. In the context of the numerical computation of complex viscoelastic flows, it is clearly unfeasible to adopt a strategy of uniform mesh refinement, in which every element of a mesh would be divided in four to generate the next more refined mesh. Instead, we have to limit ourselves to a series of meshes that are successively more refined in the critical regions of the flow domain only, namely in regions where the unknown fields develop large spatial gradients. For the case of the 4:1 contraction, the critical region is the neighborhood of the re-entrant corner. We have listed in Table 1, for each mesh, the transversal

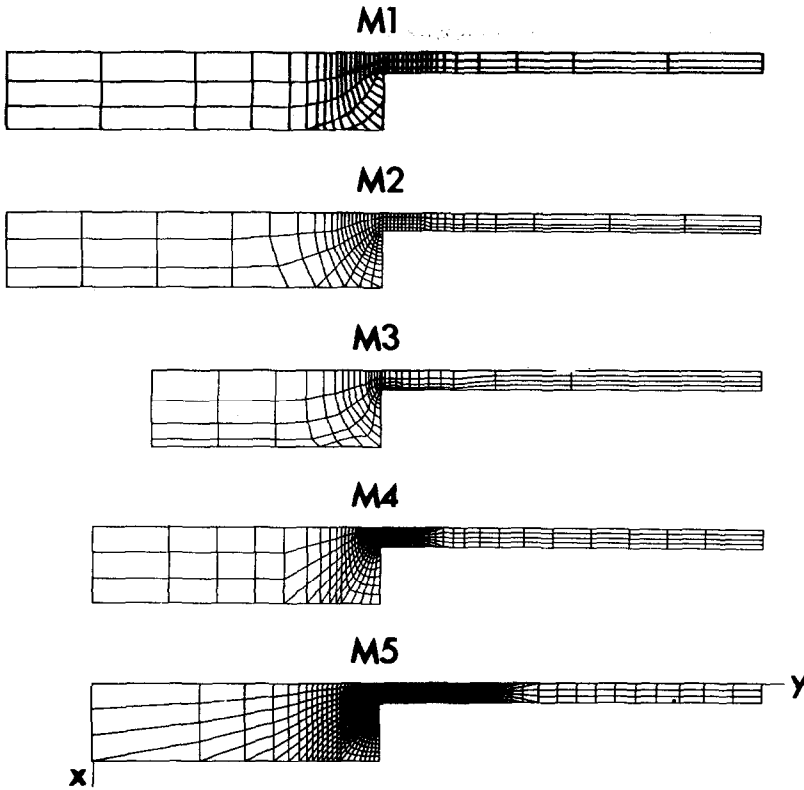


Fig. 1. Meshes M1 through M5 used in the calculations. A closer view near the re-entrant corner is shown in Fig. 2.

size of the small element located near the corner. This quantity can be regarded as a measure of the degree of refinement of our five meshes. We have taken much care in the design of M5 so as to avoid sudden steps in element size or unfavorable element aspect ratios. M5 exemplifies the notion of intensive local mesh refinement so conveniently afforded by finite elements.

Most of the computations have been conducted on a CRAY X-MP vector supercomputer. A few runs have been repeated for comparison purposes on an IBM 3081/K, a high speed scalar machine. Table 1 shows the CPU cost for a single Newton-Raphson iteration performed on the CRAY X-MP, as a function of the mesh. These figures correspond to a vectorized version of our code which does not exploit the multiprocessing environment of the CRAY X-MP. The speed ratio between the CRAY X-MP and the IBM 3081/K depends significantly upon the degree of vectorization achieved on a given mesh; it varies in the present application between 8 (with M1) and 30 (with

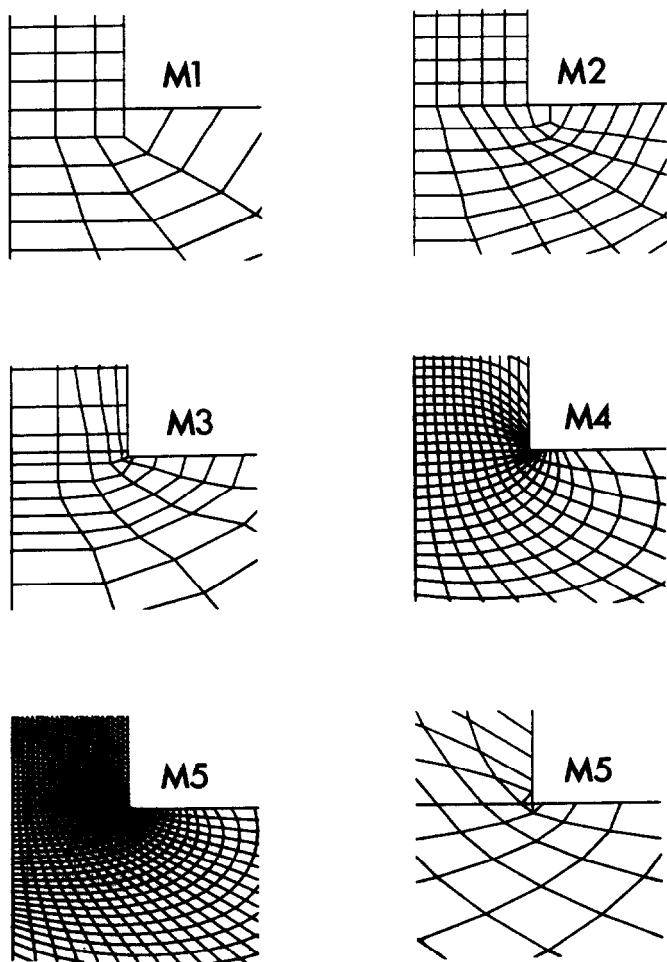


Fig. 2. Mesh configuration near the re-entrant corner for meshes M1 through M5. A further magnification is given for M5.

TABLE 1

Characteristic data of the finite element meshes

Mesh	Degrees of freedom	Size of the corner element	CPU time (s)
M1	3139	0.25	3.7
M2	5059	0.20	7.8
M3	3046	0.05	3.8
M4	11172	0.02	27.4
M5	40974	0.005	167

M5). The total cost of the computations reported in Section 3 amounts to 20 CPU hours on the CRAY X-MP, which would roughly translate into 20 days on the IBM 3081/K and a year on a VAX 11/780. We mention finally that the very large number of nodal unknowns with M5 calls for careful i/o procedures during the frontal elimination process. Indeed, the triangulated Jacobian matrix fills up about 96 Megabytes of storage in this case, to be written to and read from disk at each Newton-Raphson iteration.

3. Numerical results

We have computed viscoelastic solutions with meshes M1 to M5 for two particular cases of the Giesekus fluid: the upper-convected Maxwell fluid and the Leonov-like fluid. Before discussing these results, we briefly consider the numerical solutions obtained for a Newtonian fluid.

3.1. Newtonian fluid: $\alpha = We = 0$

In the case of a Newtonian fluid, the numerical scheme described in Section 2 allows us to choose arbitrary values for the viscosity ratio β . We have used the values $\beta = 0$ and 1, which yield the classical *mixed* and *displacement* formulations of the Stokes problem, respectively [4]. The computations do not present particular difficulties with either technique, save approximation problems near the re-entrant corner. More precisely, convergence of the numerical solutions with mesh refinement is observed everywhere in the flow domain *except* in the small corner elements, where the continuous representation (6) for the unknown fields fails to reproduce the singular behavior of the exact solution accurately.

We present in Table 2 numerical values for the Couette correction δp_{en} defined by

$$\delta p_{en} = (\Delta p - \Delta p_{fd}) / 2\tau_w, \quad (10)$$

where Δp is the calculated pressure drop in the contraction, Δp_{fd} is the

TABLE 2

Couette correction for a Newtonian fluid

Mesh	Couette correction	
	Displacement method	Mixed method
M1	0.369	0.356
M3	0.375	0.372
M5	0.374	0.374

pressure loss which would be obtained on the basis of fully developed flow in the upstream and downstream channels, and τ_w is the fully developed wall shear stress in the downstream channel. Inspection of these values reveals the consistency of the results obtained with the mixed and displacement techniques as the mesh is refined. We also note that there is no need in the Newtonian case for a highly refined mesh like M5 to obtain an accurate estimate of a global quantity such as a pressure correction.

3.2. Maxwell fluid: $\alpha = \beta = 0$

With each of the five meshes M1 to M5, a family of solutions parameterized by We has been computed up to a critical value \overline{We} . Every attempt to obtain convergent iterates for $We > \overline{We}$ failed, whatever the magnitude of the increments of We that were used in the continuation procedure. In addition, the sign of the determinant of the Jacobian matrix oscillated during these unsuccessful iterations, which implies the singularity of the Jacobian matrix in the neighborhood of \overline{We} . These facts indicate the presence of a limit point of the discrete solution families.

Our best available estimates of the location We_{lim} of this limit point in the parameter space are listed in Table 3 for the five meshes. We define We_{lim} as $\overline{We} + \Delta\overline{We}/2$, where $\Delta\overline{We}$ is the smallest increment of We used in the unsuccessful attempts to pursue the calculations beyond \overline{We} . As seen from Table 3, $\Delta\overline{We}$ is less than 10^{-2} for the five meshes. It is tempting to conclude from the results obtained with meshes M1 to M4 that the values of We_{lim} are sufficiently stable to mesh refinement to establish the presence of a limit point of the continuous problem. The use of our most refined mesh, however, clearly does not substantiate such a conclusion. The critical value of We is in this case frustratingly low. Viewed from another perspective, this shows that very intensive mesh refinement does not solve the high Weis-

TABLE 3

Location of the limit point for a Maxwell fluid; the uncertainty is defined in the text by $\Delta\overline{We}/2$

Mesh	Location We_{lim} of the limit point	Uncertainty
M1	0.873	0.00008
M2	0.565	0.0005
M3	0.556	0.0005
M4	0.588	0.0025
M5	0.112	0.0042

senberg number problem, at least in the present application and with the present numerical technique.

We now turn to the analysis of the quality of our numerical solutions. First, we wish to emphasize that the streamlines are well-behaved (namely, oscillation-free) in all the simulations reported in this paper. The same statement does not generally hold for the velocity and extra-stress fields. Clearly, inspection of the streamlines alone is not sufficient to assess the quality of viscoelastic computations.

With each of our five meshes, solutions for values of We sufficiently

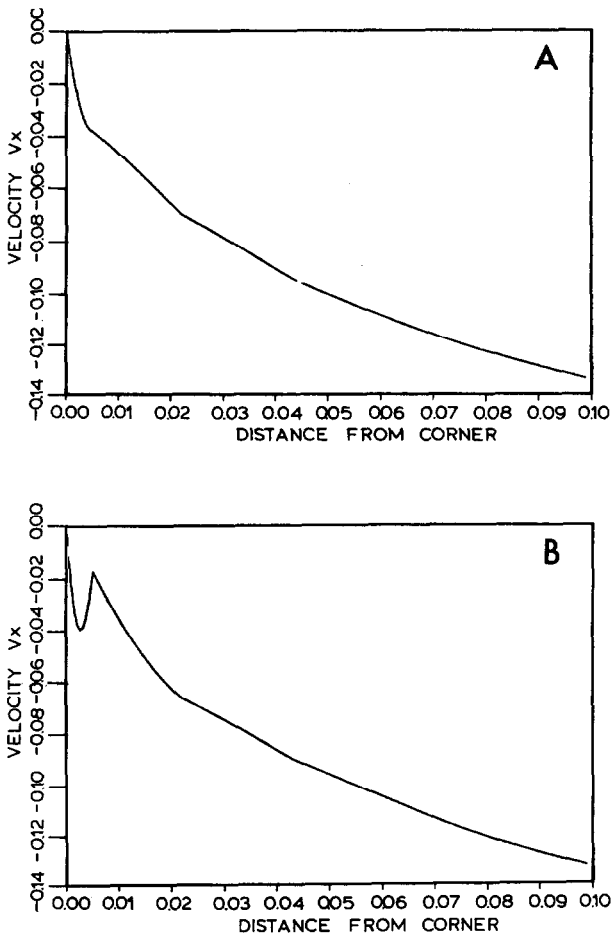


Fig. 3. Velocity v_x along the entry section of the small channel as a function of the distance from the re-entrant corner (mesh M5). (A) Newtonian solution obtained with the mixed technique, (B) solution for a Maxwell fluid at $We = 0.1083$.

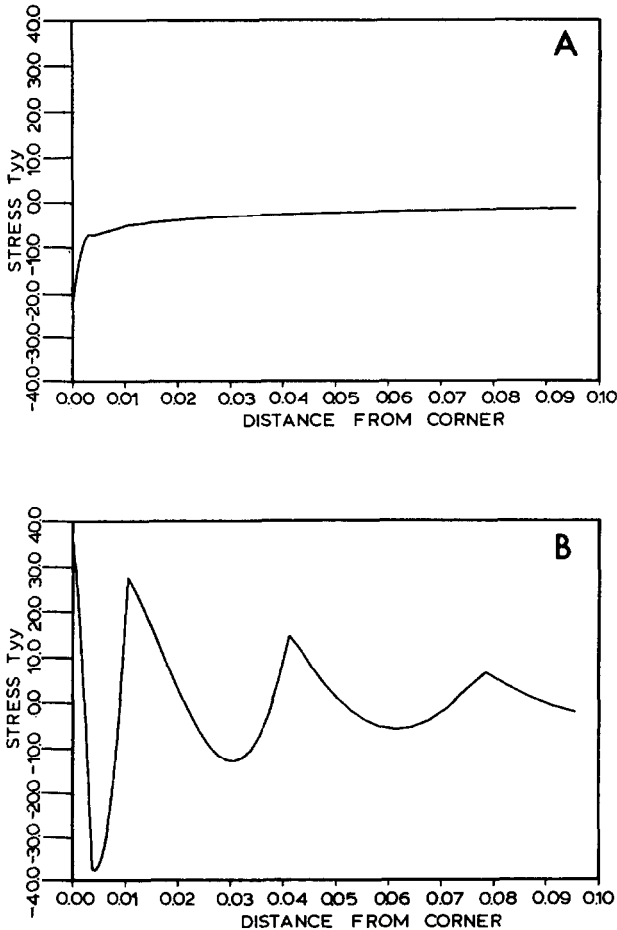


Fig. 4. Extra-stress T_{yy} along the entry section of the small channel (mesh M5). (A) Newtonian solution obtained with the mixed technique, (B) solution for a Maxwell fluid at $We = 0.1083$.

smaller than the critical value are smooth. When We is incremented towards We_{lim} , however, spurious oscillations appear in the velocity and extra-stress fields near the re-entrant corner. This is illustrated in Figs. 3 and 4, where dimensionless velocity and extra-stress profiles obtained with M5 are shown along the entry section of the small channel. In this case, the critical value \overline{We} is so small (0.1083) that contour lines of the velocity field hardly show any oscillations at all. The very close look near the re-entrant corner provided in Fig. 3b reveals, however, the presence of a spurious bump in the corner element. This significantly impairs the approximation of the spatial gradients of the velocity field near the corner. The extra-stress field calculated at \overline{We}

exhibits violent oscillations generated, again, at the corner. These numerical difficulties experienced in flow regions where the velocity and stress fields develop large spatial gradients are typical of viscoelastic computations with presently available discretization methods [4,8].

3.3 Leonov-like fluid: $\alpha = 1/2$, $\beta = 1/9$

We have performed the same mesh refinement analysis with the Leonov-like fluid. The numerical difficulties appeared to be much less pronounced in this case than with the Maxwell fluid. The presence of a purely viscous term in the discretized momentum equations (8) has a definitive stabilizing effect on the numerical results, and shear-thinning behavior tends to reduce stress levels in regions of high velocity gradients. This is consistent with our previous investigations [11,17,18].

Nevertheless, a limit point of the discrete equations (7–9) has again been encountered with all our five meshes. The location of this limit point is given in Table 4 as a function of the mesh. We see that, proceeding from M1 to M3, increasingly higher values of We can be reached. This behavior of the present numerical scheme is similar to what we have observed with the Phan Thien–Tanner fluid [18]. Based on these three sets of calculations, one might expect that further mesh refinement would displace the limit point *ad infinitum* and, consequently, solve the high Weissenberg number problem. The results obtained with M4 and M5 clearly fall short of these expectations, as seen from Table 4.

As mentioned earlier, the quality of the numerical solutions obtained with the Leonov-like fluid is significantly better than for the case of the Maxwell fluid. We show in Fig. 5 velocity and extra-stress profiles along the entry section of the small channel, obtained with M3 at $We = 4.54$. The calculated velocity field is very smooth, even for this relatively high value of We . The extra-stress field, however, exhibits spurious oscillations close to the re-en-

TABLE 4
Location of the limit point for a Leonov-like fluid

Mesh	Location We_{lim} of the limit point	Uncertainty
M1	0.805	0.005
M2	1.05	0.05
M3	4.545	0.005
M4	0.408	0.0025
M5	0.610	0.0031

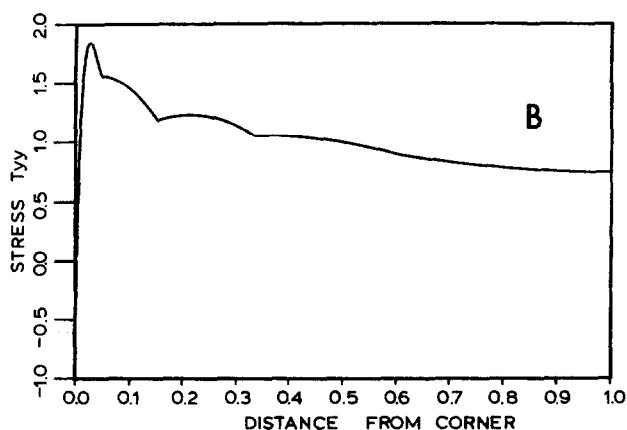
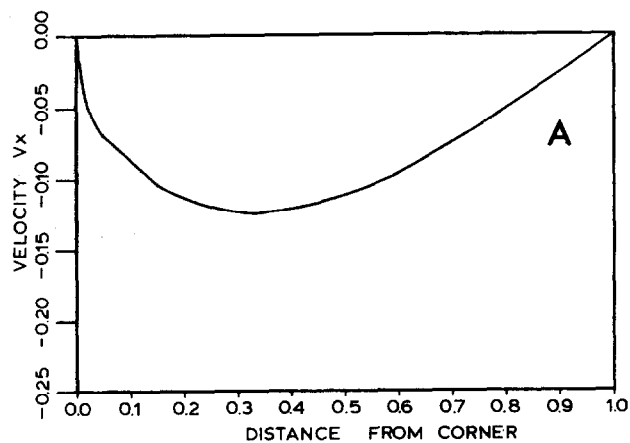


Fig. 5. Velocity and elastic extra-stress profiles along the entry section of the small channel. Results obtained for a Leonov-like fluid (mesh M3, $We = 4.54$).

trant corner. Note that the calculated stress levels are much lower than for the Maxwell fluid.

The reader may wonder what the results look like in the present application once a discrete solution family has turned back on itself at a limit point. The answer can be found in Fig. 6, where we show solutions for the Leonov-like fluid obtained with M2. Figure 6a shows the results obtained at $We = 0.025$, the initial guess for the iterative scheme being the Newtonian solution. The calculated unknown fields are smooth, and for such a small value of We , are practically identical to the Newtonian results. On the other hand, Fig. 6b shows the solution obtained *for the same value of We* , but on

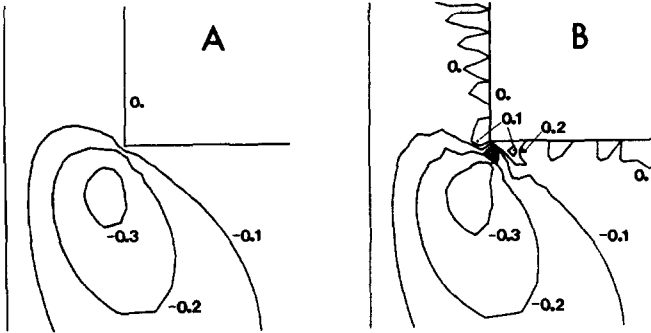


Fig. 6. Multiple solutions obtained for a Leonov-like fluid (mesh M2). (A) contour lines for the velocity v_x at $We = 0.025$; results obtained from the Newtonian solution, (B) solution for the same value of We , but obtained on the return branch.

the *return* branch. This second numerical solution is wildly oscillating, and does not, we believe, bear any resemblance to a possible exact solution of the continuous problem. Ill-behaved viscoelastic solutions calculated on the return branch have also been documented in [8,9].

4. Discussion

The results presented in Section 3 confirm the conclusions of [8,9] based on other flow problems and different numerical techniques: it is the presence of limit points in the discrete versions of viscoelastic flow problems that induces the loss of convergence of the iterative scheme beyond some critical value of the Weissenberg number. In other words, these limit points are responsible for the high Weissenberg number problem. Our very intensive mesh refinement analysis has shown, however, that the location of the limit point in the parameter space depends upon the degree of refinement of the mesh. We have observed that the quality of the discrete solutions deteriorates when the Weissenberg number is progressively increased towards the critical value. Furthermore, the discrete solutions obtained on the return branch, after the solution family has turned back on itself at the limit point, are ill-behaved even at low values of We and appear to be entirely spurious. These observations lead us to conclude that the limit points we have observed at the discrete level are not intrinsic properties of the continuous problem, but rather are the consequence of excessive discretization errors. To phrase it differently, the high Weissenberg number problem experienced in the present work has a definite numerical origin.

What makes flows through a sudden contraction so difficult to compute is undoubtedly the singular behavior of the velocity and stress fields at the

re-entrant corner. We do not know the nature of the singularity for commonly used viscoelastic models. At any rate, the present discretization method clearly does not properly take the singularity of the unknown fields into account. The same is true, by the way, for all numerical schemes developed so far for solving viscoelastic problems. The lack of a proper treatment of the singularity has no dramatic effect in the Newtonian case, but it might explain why the use of a very fine mesh significantly reduced the range of values of We for which viscoelastic solutions could be obtained.

An explanation for the numerical difficulties observed when We increases might be the failure of the Galerkin principle to produce stable approxima-

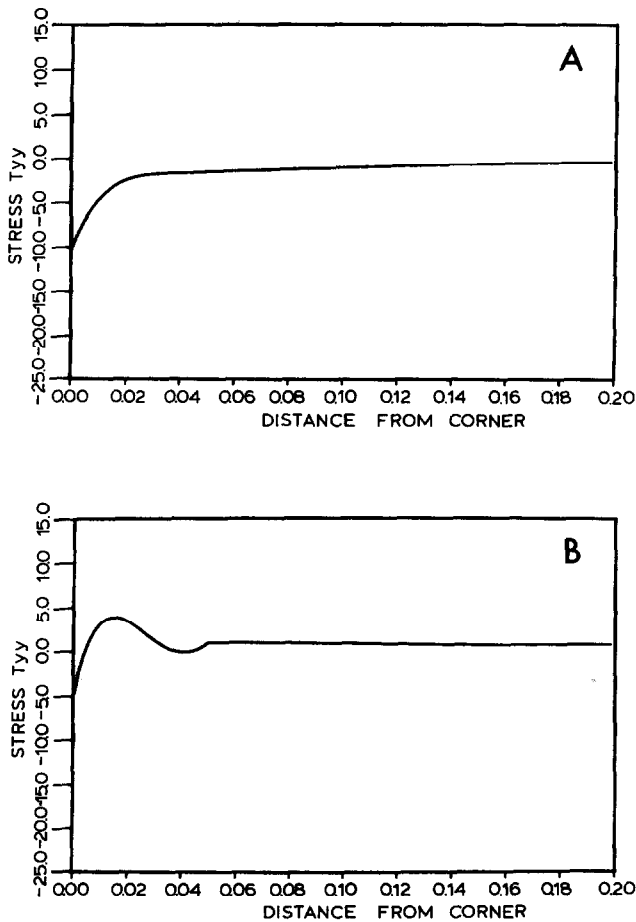


Fig. 7. Extra-stress T_{yy} along the entry section of the small channel. Results obtained for a Maxwell fluid on the basis of a Newtonian velocity field (mesh M3). (A) $We = 0$, (B) $We = 0.17$.

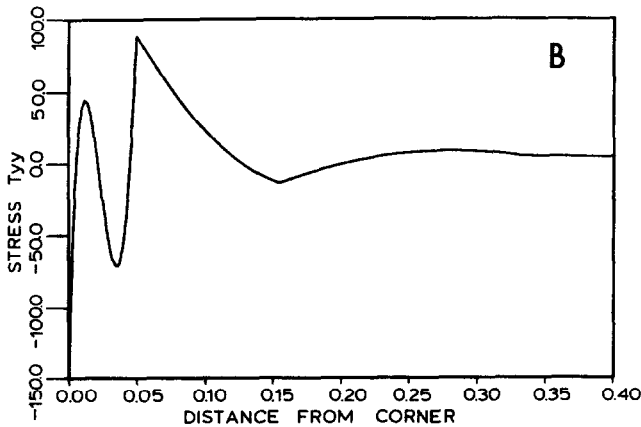
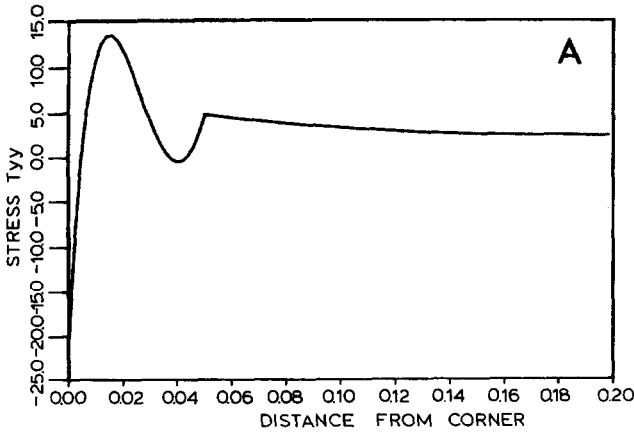


Fig. 8. Same conditions as in Fig. 7. (A) $We = 0.555$, (B) $We = 3.3$.

tions of the non-self-adjoint operators that characterize viscoelastic differential models. This type of failure has been clearly identified in the context of convection dominated transport phenomena [19]. In order to examine this question, we have solved the discrete constitutive equation (7) *alone*, given a well-behaved velocity profile (the Newtonian solution obtained by the displacement method). For the particular case of the Maxwell fluid, the reduced problem is linear in the extra-stress field and can thus be solved for any values of We . Figures 7 and 8 show solution profiles obtained with M3 along the entry section of the small channel. As in the coupled problem (7–9), results for low values of We are quite smooth, and only a very close look in the corner region reveals some discretization problems. The quality

of the solutions deteriorates, however, for higher values of We . The results obtained at $We = 3.3$ exhibit violent oscillations which propagate far away from the corner. Similar observations have been made with our most refined mesh M5 [12]. The outcome of this numerical experiment shows the limitations of the present Galerkin method and clearly points to the need for alternative discretization procedures.

5. Conclusions

The goal of this work was to identify the origin of the high Weissenberg number problem affecting the numerical solution of viscoelastic flows in complex geometries. Detailed Galerkin/Finite Element computations of the flow of Maxwell and Leonov-like fluids through a sudden contraction have shown that limit points of the discrete solution families are responsible for the loss of convergence of the iterative scheme beyond some value of the Weissenberg number. A critical examination of the numerical solutions together with a very intensive mesh refinement study have revealed, however, that these limit points are numerical artifacts caused by excessive approximation errors. We conclude that the high Weissenberg number problem experienced in the present application has a definite numerical origin. Recent studies [20,21] support the extension of our conclusion to other combinations of flow problems, constitutive models and numerical techniques.

Acknowledgments

This work was supported by the Director, Office of Energy Research, Office of Basic Energy Sciences, Materials Sciences Division of the U.S. Department of Energy under contract No. DE-AC03-76SF00098. The numerical simulations described in this paper have been conducted on a CRAY X-MP supercomputer of the National Magnetic Fusion Energy Computer Center, Lawrence Livermore National Laboratory.

References

- 1 K. Walters, *J. Non-Newtonian Fluid Mech.*, 10 (1982) 1.
- 2 R.C. Armstrong, R.A. Brown and B. Caswell, *J. Non-Newtonian Fluid Mech.*, 16 (1984) 1.
- 3 M.J. Crochet and K. Walters, *Ann. Rev. Fluid Mech.*, 15 (1983) 241.
- 4 M.J. Crochet, A.R. Davies and K. Walters, *Numerical simulation of Non-Newtonian Flow*, Elsevier, 1984.
- 5 S.L. Josse and B.A. Finlayson, *J. Non-Newtonian Fluid Mech.*, 16 (1984) 13.
- 6 O. Hassager and C. Bisgaard, *J. Non-Newtonian Fluid Mech.*, 12 (1983) 153.
- 7 R. Keunings, *J. Comp. Phys.*, 62 (1986) 199.

- 8 A.N. Beris, R.C. Armstrong and R.A. Brown, *J. Non-Newtonian Fluid Mech.*, 16 (1984) 141.
- 9 P.W. Yeh, M.E. Kim-E., R.C. Armstrong and R.A. Brown, *J. Non-Newtonian Fluid Mech.*, 16 (1984) 173.
- 10 H. Giesekus, *J. Non-Newtonian Fluid Mech.*, 11 (1982) 69.
- 11 R. Keunings, M.J. Crochet and M.M. Denn, *Ind. Eng. Chem. Fundam.*, 22 (1983) 347.
- 12 R. Keunings, Mesh refinement analysis of the flow of a Maxwell fluid through an abrupt contraction. In: C. Taylor, M.D. Olson, P.M. Gresho and W.G. Habashi (Eds.), *Numerical Methods in Laminar and Turbulent Flow, Part 2*, Pineridge Press, 1985, p. 1773.
- 13 A.I. Leonov, *Rheol. Acta*, 15 (1976) 85.
- 14 H. Giesekus, *J. Non-Newtonian Fluid Mech.*, 12 (1983) 367.
- 15 M.J. Crochet and R. Keunings, *J. Non-Newtonian Fluid Mech.*, 7 (1980) 199.
- 16 M.J. Crochet and R. Keunings, *J. Non-Newtonian Fluid Mech.*, 10 (1982) 85.
- 17 M.J. Crochet and R. Keunings, *J. Non-Newtonian Fluid Mech.*, 10 (1982) 339.
- 18 R. Keunings and M.J. Crochet, *J. Non-Newtonian Fluid Mech.*, 14 (1984) 279.
- 19 A.N. Brooks and T.J.R. Hughes, *Comput. Meths. Appl. Mech. Engrg.*, 32 (1982) 199.
- 20 J.J. Van Schaftingen and M.J. Crochet, *J. Non-Newtonian Fluid Mech.*, 18 (1985) 335.
- 21 M.J. Crochet, B. Debbaut and J.J. Van Schaftingen, *Fourth Workshop on Numerical Methods in Non-Newtonian Flow*, Spa, Belgium, 1985.